ICIC Express Letters ICIC International ©2016 ISSN 1881-803X
Volume **10**, Number **4**, April **2016** pp. **903–908**

A NEW SIDE-HOLE ACOUSTIC METHOD TO IDENTIFY CAST-IN-SITU PILES DEFECT TYPES BASED ON W-PNN

Bingxin Li[1], Huijian Li[2,*], Lixin Zhang[1] and Chen Zhang[1]

[1]Institute of Urban Construction
Hebei Normal University of Science and Technology
No. 360, Hebei Avenue, Qinhuangdao 066004, P. R. China
zhang_lx66@163.com

[2]School of Civil Engineering and Mechanics
Yanshan University
No. 438, Hebei Avenue, Qinhuangdao 066004, P. R. China
*Corresponding author: ysulhj@163.com

Received October 2015; accepted January 2016

Abstract. *In the field of identifying cast-in-situ pile defect types, a new method, i.e., optimized energy method (OEM) is proposed to overcome the low accuracy and reliability of traditional method. In OEM, wavelet transform (WT) and probabilistic neural network (PNN) are combined and used to build wavelet PNN (W-PNN), which is adopted to extract the feature energy spectrum and classify defect types, respectively. Moreover, to achieve a higher accuracy, optimized energy vector (OEV) of each signal is constructed by its energy spectrum, first amplitude and velocity. As the validation of OEM, a number of inspection signals from practical projects are applied. Experimental results indicate that the proposed method can achieve much higher identification rate (IR) than traditional method, and the increase of IR is nearly 20%.*
Keywords: Wavelet transform, PNN, Optimized energy method, Acoustic transmission method, Cast-in-situ pile, Defect type identification

1. **Introduction.** Cast-in-situ piles are widely used as building foundations for their low cost and high loading capacity. However, it is difficult to control quality during constructing process. Therefore, in the piles, sometimes there are some internal defects, such as hole, necking, mixing mud, missing vibration, which would seriously influence the safety of whole buildings. So the pile detection is usually indispensable before the next step of construction. The side-hole acoustic method is widely used in pile testing field [1]. In this method, two holes are made on two opposite sides beside a pile, acting as channels of emission sensor and receiver sensor respectively.

In traditional method, the defect types are usually identified through the first amplitude and velocity of a signal [2], but because only a small part of the signal information (first amplitude and velocity) is utilized, usually the identification accuracy is relatively low, which sometimes cannot satisfy the engineering applications. To overcome this obstacle, the study of finding more reliable methods has been a hotspot in pile nondestructive testing (NDT) field in recent years.

We all know that as a wave propagates through a defect, it would be reflected, refracted and absorbed, so the series of wave frequency band energies will attenuate. With the defect type difference, the attenuations of these series of energies are different, i.e. different frequency energy spectrums are formed. Hence, it would be a feasible way to identify a certain defect type based on its energy spectrum. So, in this paper, a new energy spectrum method is proposed. In this method, to enhance accuracy and reliability, a super information processing technology, wavelet transform (WT), is adopted to extract the feature energy spectrum from each signal firstly; and then, to realize intelligent identification, the probabilistic neural network (PNN), which is adept in pattern identification, is utilized to train and classify defect types. Furthermore, to achieve more effective results, some other useful parameters, such as first amplitude and velocity of a signal, are also joined in the frequency energy spectrum to construct corresponding optimized energy vector (OEV), which is used as the input of PNN. Therefore, this proposed method can be named optimized energy method (OEM). Experimental results indicate that these measures can successfully enhance the identification accuracy and reliability. It should be pointed out that the acoustic signals adopted in this paper are acquired in practical inspection projects of Qinhuangdao Pile Quality Test Center in recent years, and the exact types of them have been confirmed through other inspection approaches. The total identification procedures are shown in Figure 1.

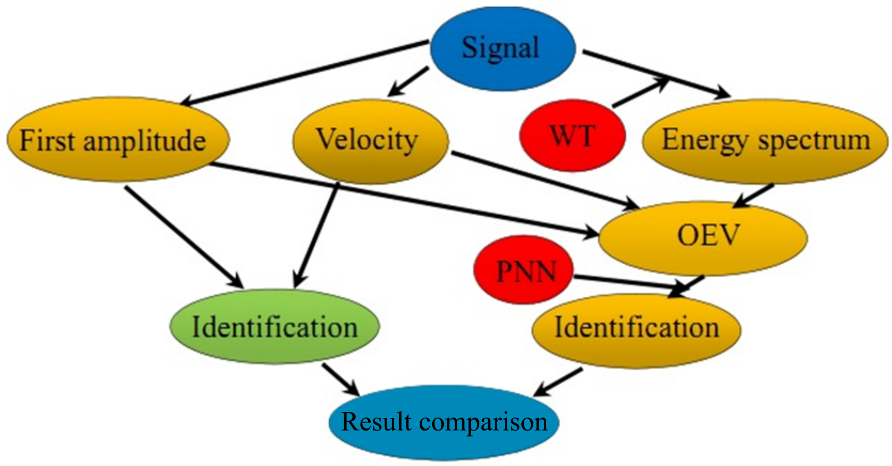

FIGURE 1. Overall flowchart of pile defect type identification

The rest of the paper is organized as follows. In Section 2, the theoretical basis (WT and PNN) is introduced briefly, and the theory of OEM (W-PNN) is proposed. In Section 3, the construction method of OEV is presented in detail. In Section 4, experimental valuation is given, including the comparison results of the traditional method and OEM, and finally some conclusions are drawn in Section 5.

2. **W-PNN.** WT is versatile in feature extraction and has been applied in identification and selection as a terrific trait extraction tool in many fields [3]. A family of time-scale waveforms can be expressed

$$\psi_{a,b}(t) = a^{-1/2}\psi\left(\frac{t-b}{a}\right), \quad a > 0,\ b \in R \tag{1}$$

where $\psi(t)$ is a wavelet function which satisfies equation $\int_R \psi(t)\mathrm{d}t = 0$, a is the scale parameter and b is the time parameter. The WT of an arbitrary function $x \in L^2$ can be given by Equation (2).

$$\int_R f(t)\cdot\psi_{a,b}(t)\mathrm{d}t = a^{-1/2}\int_R f(t)\cdot\psi\left(\frac{t-b}{a}\right)\mathrm{d}t \tag{2}$$

The width and location of time frequency window change corresponding to the changes of a and b, i.e., the size and location of time frequency window are variable. WT also permits to decompose a signal in many levels [4], as shown in Figure 2. In each level, the signal is decomposed into approximation part and detail part with the use of low-pass filter and high-pass filter. Hence, WT can provide a multi-scale and multi-resolution analysis.

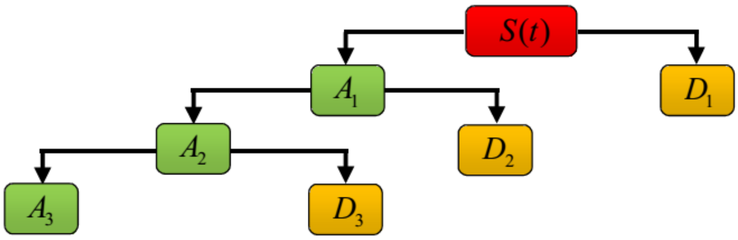

FIGURE 2. Tree of wavelet transform

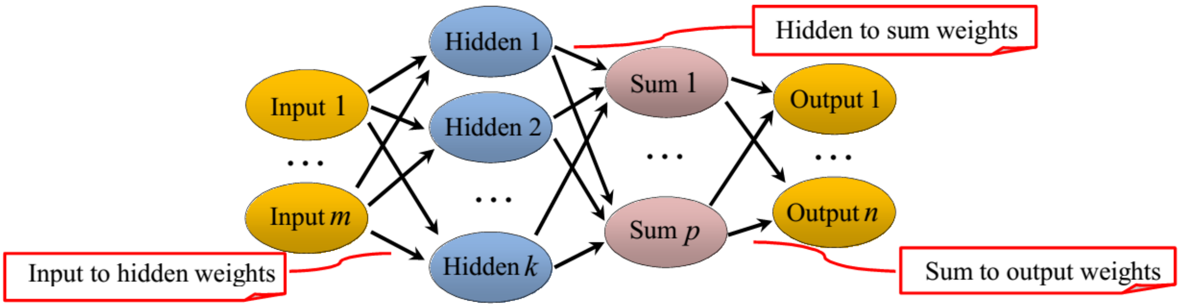

FIGURE 3. Model of PNN

PNN is a kind of self-monitoring neural network, whose theory basis is Bayesian minimum risk criteria [5]. The PNN model is composed of four layers: input layer, pattern layer, summation layer and output layer whose functions are receiving input vectors, calculation, data summation and outputting results, respectively. Its model is shown in Figure 3.

Through Equation (3), the output of each unit in the pattern layer is calculated.

$$\Phi_{ij}(x) = (2\pi)^{-0.5d}\sigma^{-d} \exp\left[-\frac{(x-x_{ij})^T(x-x_{ij})}{2\sigma^2}\right] \tag{3}$$

where $i = 1, \cdots, M$, $j = 1, \cdots, N$, M is the total number of classes in the training samples, x_{ij} is the jth mode, N is the number of neurons in the pattern layer of the PNN ith class, σ and d are the smooth parameter and the data dimension of the samples. The summation layer is the cumulative probability belonging to a certain class, which is calculated through Formula (4).

$$f_{iN_i}(x) = N_i^{-1}\sum_{j=1}^{N_i}\Phi_{ij}(x) \tag{4}$$

Compared with other neural networks, the convergence speed of PNN is much faster and the recognition is more effective [6]. In this paper, WT and PNN are combined and used to build wavelet-probabilistic neural network (W-PNN). In W-PNN, WT is adopted to extract feature energy spectrum and PNN to train and identify. Its model is shown in Figure 4.

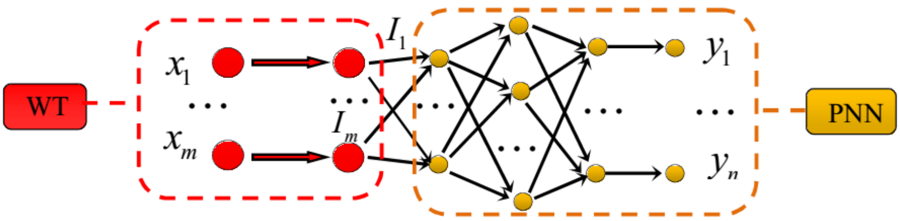

FIGURE 4. Structure of W-PNN

As shown in Figure 4, the series of $x_1, \cdots, x_m$ are the series of original input signals, the series of $I_1, \cdots, I_m$ are the series of constructed energy vectors and the series of $y_1, \cdots, y_n$ are the series of output results.

3. **Construction of OEV.**

Suppose a_i is the amplitude of ith point of a signal $S(t)$, its energy can be calculated through Formula (5).

$$E = \int |S(t)|^2 \mathrm{d}t = \sum_{i=1}^{n} |a_i|^2, \quad i = 1, 2, \cdots, n \tag{5}$$

Similarly, the energies of sub-signals $(A_1, D_1, A_2, D_2, A_3, D_3, \cdots)$ can also be calculated through Formula (5).

The average amplitude AA of a signal can be calculated through the following formula:

$$AA = \sum_{i=1}^{n} |a_i|, \quad i = 1, 2, \cdots, n \tag{6}$$

where a_i is the amplitude of the ith point of the signal. Suppose the distance between the emission sensor and the receiver sensor is l, the propagation time of the wave is t, then the velocity: $V = l/t$.

To achieve easy convergence of W-PNN, all elements of the OEV are processed into relative values. Through lots of experiment validations, we notice that the differences between defect signals and no-defect signals (the signals that propagate through good quality concrete material) are significant in identifying defect types. So, in this paper, the OEV of a signal is designed as Formula (7).

$$I = \left[\frac{AA^* - AA}{(AA^* - AA)_{\max}}, \frac{V^* - V}{(V^* - V)_{\max}}, \frac{E_1^* - E_1}{(E_1^* - E_1)_{\max}}, \frac{E_2^* - E_2}{(E_2^* - E_2)_{\max}}, \cdots, \frac{E_k^* - E_k}{(E_k^* - E_k)_{\max}} \right] \tag{7}$$

where $AA^*, V^*, E_1^*, E_2^*, \cdots, E_k^*$ are the average amplitude, velocity and a series of energy spectrum of a no-defect signal, and $AA, V, E_1, E_2, \cdots, E_k$ are those of a defect one respectively.

4. **Experiment and Valuation.**

The entire inspection system diagram is shown in Figure 5. During testing, the emission sensor and receiver sensor always keep the same elevation as they move from bottom to top of a pile.

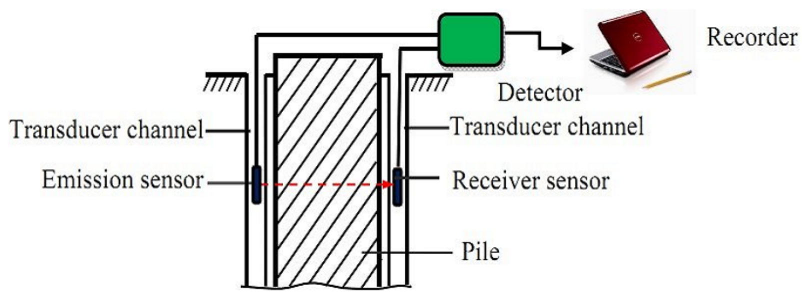

FIGURE 5. Total inspection system diagram of testing

4.1. **Identification results of traditional method.**

In traditional method, the first amplitude and wave velocity of a signal are acquired firstly, and the type identification is based on them. The identification results are listed in Table 1.

From Table 1, we noticed that the identification rates (IRs) range from 56.0% to 66.0%, which are relatively low, so this method is usually not satisfied in engineering applications.

Table 1. Identification results of traditional method

Defect type	Hole	Necking	Mixing mud	Missing vibration
Misjudgment	6	5	2	4
Failure	10	9	9	7
Identification	31	20	14	15
Identification rate	66.0%	58.8%	56.0%	57.7%

4.2. **Identification results of OEM.** In OEM, the first amplitude and wave velocity of each signal are also utilized. The wavelet functions and the number of decomposition levels are adjusted according to the extraction effects. Finally, the function $db5$ and 3 level are adopted. The energies of sub-signals D_1, D_2, D_3, A_3 are E_1, E_2, E_3, E_4, respectively. Part of OEVs of all type defects are listed in Table 2.

Table 2. Part of OEVs

Defect type		Hole	Necking	Mixing mud	Missing vibration	Element serial number
$(AA^* - AA)\,/\,(AA^* - AA)_{\max}$		0.651	0.8043	1.0000	0.9428	1
$(V^* - V)/(V^* - V)_{\max}$		0.8436	0.9533	1.0000	0.8976	2
Energy spectrum	$(E_1^* - E_1)\,/\,(E_1^* - E_1)_{\max}$	1.0000	0.9742	0.2406	0.3745	3
	$(E_2^* - E_2)\,/\,(E_2^* - E_2)_{\max}$	0.2895	0.4672	0.3164	1.0000	4
	$(E_3^* - E_3)\,/\,(E_3^* - E_3)_{\max}$	0.7519	0.6787	1.0000	0.4687	5
	$(E_4^* - E_4)\,/\,(E_4^* - E_4)_{\max}$	0.8359	1.0000	0.9421	0.7862	6

To present OEVs more directly, a column chart is illustrated in Figure 6.

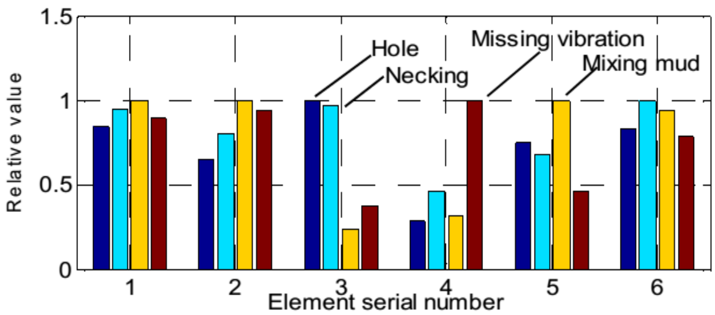

Figure 6. Energy column chart of OEVs

As shown in Figure 6, the proportional distributions of the OEV elements of these four type defects are different, so it is a feasible approach to classify defect types with the use of W-PNN. In next stage, the parameters of the W-PNN are also adjusted based on the identification results, and finally identification results are listed in Table 3. From Table 3, we also noticed that the IRs of OEM range from 76.0% to 85.1%, which are much higher than those of the traditional method.

Table 3. Identification results of OEM

Defect type	Hole	Necking	Mixing mud	Missing vibration
Misjudgment	3	2	1	2
Failure	4	5	5	4
Identification	40	27	19	20
Identification rate	85.1%	79.4%	76.0%	76.9%

5. **Conclusions.** In this paper, OEM is proposed in the field of cast-in-situ pile defect type identification. In the proposed method, WT and PNN are combined and used to construct W-PNN, and OEV of each signal is constructed by its energy spectrum, first amplitude and wave velocity to enhance the identification accuracy. Experimental results indicate that the proposed method has great advantages over traditional one, and the accuracy is increased up to nearly 20%, as shown in Table 1 and Table 3. However, we also notice that the IRs of some type defects are yet relatively low, such as those of mixing mud and missing vibration, which will be the focus of our next stage work.

Acknowledgment. This work is partially supported by the National Natural Science Fund (11072210) and the Province Science and Technology Support Project of Hebei (13275802). The authors also gratefully acknowledge the helpful comments and suggestions of the reviewers, which have improved the presentation.

REFERENCES

[1] G. Chu, X. Xu, T. Wu and T. Liu, Application of side-hole acoustic transmission method to non-destructive detection of driven piles, *Journal of Chongqing Jiaotong University*, vol.29, no.3, pp.450-453, 2010.

[2] M. Krause, U. Dackermann and J. Li, Elastic wave modes for the assessment of structural timber: Ultrasonic echo for building elements and guided waves for pole and pile structures, *Journal of Civil Structural Health Monitoring*, vol.5, no.2, pp.221-249, 2015.

[3] B. Abibullaev, H. D. Seo and M. S. Kim, Epileptic spike detection using continuous wavelet transforms and artificial neural networks, *International Journal of Wavelets, Multiresolution and Information Processing*, vol.8, no.1, pp.33-48, 2010.

[4] Y. Yin, L. Wang, H. Liu and Q. Fan, Rapid phase selection method on multi-resolution morphological gradient with series structure, *International Journal of Control and Automation*, vol.6, no.2, pp.255-262, 2013.

[5] W. Cui, J. Wang, J. Song and J. Gao, Fault diagnosis of polymerization kettle equipment based on probabilistic neural networks, *ICIC Express Letters, Part B: Applications*, vol.6, no.7, pp.1767-1772, 2015.

[6] V. J. Larin and E. E. Fedorov, Combination of PNN network and DTW method for identification of reserved words, used in aviation during radio negotiation, *Radioelectronics and Communications Systems*, vol.57, no.8, pp.362-368, 2014.